Submitted to ApJ Letters
Preprint typeset using LaTeX style emulateapj v. 25/04/01

BAR EVOLUTION OVER THE LAST EIGHT BILLION YEARS: A CONSTANT FRACTION OF STRONG BARS IN GEMS

Shardha Jogee[1], Fabio D. Barazza[1], Hans-Walter Rix[2], Isaac Shlosman[3], Marco Barden[2], Christian Wolf[4], James Davies[1], Inge Heyer[1], Steven V.W. Beckwith[1,5], Eric F. Bell[2], Andrea Borch[2], John A. R. Caldwell[1], Christopher J. Conselice[6], Tomas Dahlen[1], Boris Häussler[2], Catherine Heymans[2], Knud Jahnke[7], Johan H. Knapen[8], Seppo Laine[9], Gabriel M. Lubell[10], Bahram Mobasher[1], Daniel H. McIntosh[11] Klaus Meisenheimer[2], Chien Y. Peng[12], Swara Ravindranath[1], Sebastian F. Sanchez[7], Rachel S. Somerville[1] and Lutz Wisotzki[7]

Submitted to ApJ Letters

ABSTRACT

One third of present-day spirals host optically-visible strong bars that drive their dynamical evolution. However, the fundamental question of how bars evolve over cosmological times has yet to be addressed, and even the frequency of bars at intermediate redshifts remains controversial. We investigate the frequency of bars out to $z \sim 1$ using 1590 galaxies drawn from the GEMS survey, which provides morphologies from *Hubble Space Telescope* Advanced Camera for Surveys (ACS) two-color images, and accurate redshifts ($\delta_{\rm z}/(1+z) \sim 0.02$ down to $R_{\rm Vega}$= 24) from the the COMBO-17 survey. We identify spiral galaxies using three independent techniques based on the Sersic index, concentration parameter, and rest-frame color. We characterize bar and disk features by fitting ellipses to F606W and F850LP images, taking advantage of the two bands to minimize bandpass shifting. We exclude highly inclined ($i > 60°$) galaxies to ensure reliable morphological classifications, and apply different completeness cuts of $M_{\rm V} - 5 \log h \leq -18.5$ and -19.9. More than 40% of the bars we detect have semi-major axes $a < 0.5''$ and would be easily missed in earlier surveys without the small PSF of ACS. The bars we can reliably detect are fairly strong (with ellipticities $e \geq 0.4$) and have a in the range $\sim$ 1.2–13 kpc. We find that the optical fraction of such strong bars shows no sign of a drastic decline at $z > 0.7$, but remains at $\sim 30\% \pm 6\%$ at lookback times of 2–6 Gyr ($z \sim 0.2$–0.7), 6–8 Gyr ($z \sim 0.7$–1.0), and the present-day. Our findings of a large and similar bar fraction at these three epochs favor scenarios where cold gravitationally unstable disks are already in place by $z \sim 1$, and where on average bars have a long lifetime (well in excess of 2 Gyr). We note, however, that the distributions of bar properties in the two slices are not statistically identical and allow, therefore, for the possibility that the bar strengths and sizes may evolve over time.

Subject headings: galaxies: general — galaxies: spiral — galaxies: structure — galaxies: evolution

1. INTRODUCTION

It is widely recognized that stellar bars, either spontaneously or tidally-induced, redistribute mass and angular momentum and thereby drive the dynamical and secular evolution of galaxies (e.g., Pfenniger & Norman 1990; Shlosman, Frank, & Begelman 1989; Friedli & Martinet 1993; Friedli & Benz 1993; Kormendy & Kennicutt 2004). In the local Universe, one third of local spiral galaxies host optically-visible strong bars (e.g., Eskridge et al. 2002, hereafter ES02; see also § 3). Mounting evidence, including observations of central molecular gas concentrations (e.g., Sakamoto et al. 1999), gas velocity fields (e.g., Regan, Vogel, & Teuben 1997), and circumnuclear starbursts (e.g., Hunt & Malkan 1999; Jogee, Scoville, & Kenney 2004a), suggests that bars strongly influence their host galaxies. However, the most fundamental issues on how bars form and evolve over cosmological times have yet to be resolved. When and how did bars form? Are bars a recent phenomenon or were they abundant at early cosmic epochs? Are bars short- or long-lived? In particular, do they recurrently dissolve and re-form over a Hubble time or do they represent a one-time event? How do stellar bars fit within the hierarchical clustering framework of galaxy evolution and relate to the underlying disk evolution?

The evolution of a bar is a complex process depend-

[1] Space Telescope Science Institute, 3700 San Martin Dr., Baltimore, MD 21218, U.S.A; jogee@stsci.edu
[2] Max-Planck Institute for Astronomy, D-69117 Heidelberg, Germany
[3] University of Kentucky, Lexington, KY 40506-0055, U.S.A
[4] University of Oxford Astrophysics, Oxford OX1 3RH, U.K.
[5] Johns Hopkins University, Charles and 4th Street, Baltimore, MD 21218, U.S.A
[6] CalTech, Dept. of Astronomy, Pasadena, CA 91125, U.S.A,
[7] Astrophysikalisches Institut Potsdam, D-14482 Potsdam, Germany
[8] University of Hertfordshire, Hatfield, Herts AL10 9AB, U.K.
[9] Spitzer Science Center, CalTech, Pasadena, CA 91125, U.S.A,
[10] Vassar College, Dept. of Physics and Astronomy, Poughkeepsie, NY 12604, U.S.A
[11] University of Massachusetts, Amherst, MA 01003, U.S.A
[12] University of Arizona, Tucson, AZ 85721, U.S.A

ing on the host galaxy structure, the dark matter (DM) halo, and the environment. Numerical simulations make widely different predictions on the evolution, potential dissolution, and reformation of bars over a Hubble time (e.g., Friedli & Benz 1993; Shlosman & Noguchi 1993; El-Zant & Shlosman 2002; Athanassoula 2002; Bournaud & Combes 2002; Shen & Sellwood 2004). Observationally, few and conflicting results on bars at intermediate redshifts have been published. Based on 46 moderately inclined WFPC2-imaged galaxies in the Hubble Deep Field (HDF), Abraham et al. (1999, hereafter A99) claim a dramatic decline in the rest-frame optical bar fraction ($f_{\rm opt}$) from $\sim 24\%$ at $z \sim 0.2$–0.7 to below 5% at $z > 0.7$. Based on NICMOS images of 95 galaxies in the HDF at $z \sim 0.7$–1.1, Sheth et al. (2003, hereafter S03) detect four large bars with mean semi-major axes a of 12 kpc (1.4″), while smaller bars presumably escaped detection due to the large NICMOS PSF. S03 point out that their observed bar fraction of $\sim 5\%$ for large (12 kpc) bars at $z > 0.7$ is at least comparable to the local fraction of similarly large bars. From a study based on *Hubble Space Telescope* (*HST*) Advanced Camera for Surveys (ACS) F814W images of 186 galaxies over a $3.9' \times 4.2'$ area in the Tadpole field, Elmegreen, Elmegreen, & Hirst (2004, hereafter E04) report a constant optical bar fraction of $\sim$ 20–40% at $z \sim 0$–1.1. This study is limited by the large (0.1–0.4) errors of the photometric redshifts (Benítez et al. 2004), and the small sample size precludes absolute magnitude completeness cuts at different redshifts. Furthermore, with only a single ACS filter over the range $z \sim 0$–1.1, the rest-frame bandpass of the observations shifts by more than a factor of two.

In this Letter (Paper I; see also Jogee et al. 2004b), we present the first results of an extensive study of bars at $z \sim 0.2$–1.0, based on two-color ACS images covering $14' \times 14'$ ($\sim$25%) of the GEMS[13] Survey. The area and the sample size of 1590 galaxies provide at least an order of magnitude better number statistics than earlier studies. We quantitatively identify bars using ellipse fits and minimize the effects of bandpass shifts by using both F850LP and F606W images (§ 2.2). Using the highly accurate redshifts (§ 2.1), we compare the bar fractions in two redshift slices after applying completeness criteria. We show that the optical fraction of strong (ellipticities $e \geq 0.4$) bars is remarkably constant ($\sim 30\%$) at lookback times $T_{\rm back} \sim 6$–8 Gyr ($z \sim 0.7$–1.0) [14], $T_{\rm back} \sim 2$–6 Gyr ($z \sim 0.2$–0.7), and the present-day (§ 3). Implications for galaxy evolution and future work are addressed.

2. OBSERVATIONS, SAMPLE, AND METHODOLOGY

2.1. *Observations and Sample Selection*

GEMS is a two-color (F606W and F850LP) *HST* ACS imaging survey (Rix et al. 2004) of an 800 arcmin^2 ($\sim 28' \times 28'$) field centered on the *Chandra* Deep Field South. GEMS consists of 78 one-orbit-long ACS pointings in each filter, and reaches a limiting 5σ depth for point sources of 28.3 and 27.1 AB mag in F606W and F850LP, respectively. GEMS provides high resolution ($\sim 0.05''$ or 360 pc at $z \sim 0.7$) ACS images for ~ 8300 galaxies in the redshift range $z \sim 0.2$–1.1, where accurate redshifts ($\delta_z/(1+z) \sim 0.02$ down to $R_{\rm Vega} = 24$) and SEDs based on 17 filters exist from the COMBO-17 project (Wolf et al. 2004). For this Letter, we analyze only $\sim 25\%$ of the GEMS field as this area ($14' \times 14'$) is already 30 times that of the HDF and yields good number statistics and robust results on the bar fraction (§ 3). It provides a sample that consists of 1590 galaxies in the range $z \sim 0.2$–1.0 and $R_{\rm Vega} \leq 24$. In a future paper (Jogee et al. in prep., Paper II), we will use the entire GEMS sample to compare how bar properties evolve over 8 Gyr at 1 Gyr intervals.

2.2. *Characterizing bars and $f_{\rm opt}$ out to $z \sim 1.0$*

We use two complementary methods for assessing bar properties in two redshift slices at $0.25 < z \leq 0.70$ and $0.7 < z \leq 1.0$. The first is to identify bars in the reddest filter (F850LP) at all z in order to minimize extinction and better trace the old stellar potential. However, this method (referred to as Method I in Table 1) suffers from bandpass shifting as the rest-frame band changes from I to B across the redshift range 0.2–1.0. The second complementary method is to trace bars in both F606W and F850LP images such that the rest-frame band remains relatively constant, between B and V, out to $z \sim 1.0$. Table 1 shows results based on both strategies.

We identify bars and other galactic components in F606W and F850LP images via the widely used (e.g., Wozniak et al. 1995; Jogee et al. 1999; Knapen et al. 2000; Jogee et al. 2002) procedure of fitting ellipses using the standard IRAF "ellipse" routine. We developed a wrapper that automatically runs "ellipse" for a range of different initial parameters, performing up to 200 fits per galaxy. We successfully fitted ellipses to 90% of the 1590 galaxies, while the 10% failure cases included mostly very disturbed systems where no centering could be performed, and some extended low surface brightness systems. For all fitted galaxies, we inspected the image (Fig. 1a), the fitted ellipses overlaid on the images (Fig. 1b), and the radial profiles (Fig. 1c) of intensity, ellipticity (e), and position angle (PA) in order to confirm that the best fit is reliable. This inspection was aided by a visualization tool we developed. We identify a bar as such if the fitted ellipses and radial profiles show the following characteristic bar signature (e.g, Wozniak et al. 1995) illustrated in Fig. 1. *(i)* The ellipticity (e) must rise to a *global* maximum $e_{\rm max}$, which we require to be above 0.25, while the PA has a plateau (within $\pm$ 20°) along the bar. *(ii)* Beyond the bar end, as the bar-to-disk transition occurs, e must drop by ≥ 0.1, while the PA changes by $\geq 10°$. From the profiles, we identify e, PA, and semi-major axes a of both the bar and outer disk. We quantify the bar strength using $e_{\rm max}$, which correlates locally with other measures of bar strength, such as the gravitational bar torque (Laurikainen, Salo, & Rautiainen 2002).

The sample of 1430 galaxies with successful ellipse fits includes galaxies of different morphological types (disks and spheroids), inclinations, and absolute magnitudes. We apply two cuts at $M_{\rm V} - 5 \log h \leq -18.5$ and -19.9. The first cut gives us a sizeable sample of galaxies with a range of absolute magnitudes (-18.5 to -23.0) similar to that of the Ohio State University (OSU) survey, which

[13] Galaxy Evolution from Morphology and SEDs (spectral energy distributions).

[14] We assume a flat cosmology with $\Omega_M = 1 - \Omega_\Lambda = 0.3$ and $H_0 = 100 \times h$ km s^{-1} Mpc^{-1}, where $h = 0.7$ throughout this paper.

is used to define the local bar fraction (ESO2). However, K-corrections based on local Scd templates (Coleman, Wu, & Weedman 1980) suggest that we are only complete out to $z \sim 0.8$ for the first cut. The second more stringent cut at -19.9 ensures completeness out to $z \sim 1.0$, but it reduces the sample drastically (see Table 1). In addition, to ensure reliable bar detection, we use the disk inclination i from ellipse fits (§ 2.2) to exclude highly inclined ($i > 60°$) galaxies.

The optical bar fraction $f_{\rm opt}$ is defined as $N_{\rm bar}/N_{\rm sp-disk}$, where $N_{\rm sp-disk}$ is the number of spiral or disk galaxies, and $N_{\rm bar}$ is the number of such systems hosting bars. We identify spiral/disk galaxies using three independent techniques (Table 1). We first use the criterion $n < 2.5$, where n is the index of single-component Sersic models fitted to GEMS galaxies (Häussler et al. in prep.) with the GALFIT (Peng et al. 2002) package. Our choice of $n < 2.5$ is dictated by the fact that a study of GEMS galaxies at $z \sim 0.7$ (Bell et al. 2004), as well as tests where we insert artificial galaxies in the GEMS fields, suggest that a Sersic cut of $n \leq 2.5$ picks up disk-dominated systems. The second technique uses a cut $C < 3.4$, where C is the CAS (Conselice et al. 2000) concentration index. Thirdly, we use rest-frame $U - V$ color cuts in the range 0.8–1.2 to broadly separate spiral galaxies from red E/S0s, based on local SED templates (Coleman et al. 1980) and the observed red sequence at $z \sim 0.7$ (Bell et al. 2004). The third method is least robust as the effects of dust and aging stellar populations reduce the effectiveness of $U - V$ cuts in separating spirals and E/SOs.

3. RESULTS AND DISCUSSION

The bars we identify primarily have ellipticities $e \geq 0.4$ (Fig. 2a) and semi-major axes a in the range $0.15''$–$2.2''$ (Fig. 2b) and 1.2–13 kpc (Fig. 2c). Our experiment of artificially redshifting B-band images of a subset of OSU galaxies out to $z \sim 1$ shows that it is difficult to unambiguously identify weaker ($e \leq 0.3$) bars, and we limit the discussion in this paper to strong ($e \geq 0.4$) bars. Table 1 shows the optical bar fraction $f_{\rm opt}$ of such bars in the two redshift slices ($0.25 < z \leq 0.70$ and $0.7 < z \leq 1.0$) derived in the reddest filter and in a relatively fixed rest-frame band (§ 2.2). Results for $M_{\rm V} - 5 \log h \leq -18.5$ are shown, based on 627 galaxies out of which we identify 258 moderately inclined ($i < 60°$) spirals that host ~ 80 bars. The consistency in the six entries attests to the robustness of the results, and shows that the fraction of optically-visible bars remains in the range 23%–36% or at $\sim 30\% \pm 6\%$ in both slices. Incompleteness effects (§ 2.2) do not bias the results since the cut at -19.9 gives similar bar fractions, shown in brackets (Table 1). The bar fraction is slightly higher in the rest-frame I-band than B-band, possibly indicative of dust and SF masking bars at bluer wavelengths. Our findings of a fairly constant $f_{\rm opt}$ are consistent with E04 and do not show the dramatic decline in $f_{\rm opt}$ reported by A99.

More than 40% of the bars we detect have semi-major axes $a < 0.5''$ (Fig. 2b) and may be missed in earlier WFPC2 and NICMOS surveys that did not benefit from the small ($0.05''$) ACS pixels, and the resulting narrow PSF. Several factors, such as the wider PSF, low number statistics, cosmic variance, and methodology may have led to the lower $f_{\rm opt}$ reported by A99, but we cannot address this issue in more detail as the coordinate list of galaxies in that study is not published.

How do our results compare to $f_{\rm opt}$ for correspondingly strong bars in the local Universe? There are as yet no statistics published on $z \sim 0$ bars based on a large volume-limited sample such as SDSS. As the next best alternative, we turn to the OSU sample (ES02). For $i < 60°$ spirals, we find $f_{\rm opt} \sim 37\%$ for strong bars classified according to the visual RC3 'SB' bar class, and $f_{\rm opt} \sim 33\%$ for strong bars classified according to $e \geq 0.4$, where e is based on ellipse fits to OSU B-band images. Thus, *it appears that the optical fraction of strong ($e \geq 0.4$) bars remains remarkably similar at $\sim$ 30%–37% at lookback times of $\sim$ 6–8 Gyr ($z \sim$ 0.7–1.0), $\sim$ 2–6 Gyr ($z \sim$ 0.2–0.7), and at the present-day.* Our findings have several implications for disk and bar evolution. *(i)* The abundance of strong bars at early times implies that dynamically cold disks that can form large-scale stellar bars are already in place by $z \sim 1$. They also suggest that highly triaxial, centrally concentrated DM halos, which tend to destabilize the bar (El-Zant & Shlosman 2002), may not be prevalent in galaxies at $z \sim$ 0–1. *(ii)* The remarkably similar fraction of strong bars at lookback times of 6–8 Gyr, 2–6 Gyr, and in the present day support the view that large-scale stellar bars are long-lived (e.g., Athanassoula 2002; Shen & Sellwood 2004; Martinez-Valpuesta, Shlosman & Heller 2004), with a lifetime well above 2 Gyr. *(iii)* We note that a similar *fraction* of bars at different epochs does not exclude the possibility that the bar strength (ellipticity) and its size can evolve in time due to intrinsic factors and concurrent changes in the surrounding disk, bulge and halo potentials (e.g., Athanassoula 2002; Martinez-Valpuesta & Shlosman 2004). Kolmogorov-Smirnov ($K-S$) tests on the distributions of e and a for different magnitude cuts (-18.5, -19.0, and -19.9) yield primarily P in the range 0.2–0.5, where P is the significance level for the null hypothesis that the two data sets are drawn from the same distribution. Such values of P hint at possible evolutionary effects but are inconclusive, and a larger sample is needed. While this Letter focuses on the bar *fraction* , in Paper II (Jogee et al., in prep.), we will invoke the full GEMS sample of 8300 galaxies to compare the bar properties (e.g., strengths and bar sizes normalized by disk sizes) with host galaxy properties (e.g., disk scale lengths, masses, and B/D ratios) over the last 8 Gyr at 1 Gyr intervals.

SJ, FDB, IS, and DHM acknowledge support from NASA/LTSA/ATP Grants NAG5-13063, NAG5-13102, and ATP 5-10823, and NSF AST-0206251. EFB and SFS acknowledge support from ECHPP under HPRN-CT-2002-00316, SISCO and HPRN-CT-2002-00305, Euro3D RTN. CW was supported by a PPARC Advanced Fellowship. Support for the GEMS was provided by NASA through GO-9500 from STScI, which is operated by AURA for NASA, under NAS5-26555.

REFERENCES

Abraham, R. G., Merrifield, M. R., Ellis, R. S., Tanvir, N. R., & Brinchmann, J. 1999, MNRAS, 308, 569 (A99)
Athanassoula, E. 2002, ApJL, 569, L83
Bell, E. F., et al. 2004, ApJL, 600, L11
Benítez, N., et al. 2004, ApJS, 150, 1
Bournaud, F. & Combes, F. 2002, A&A, 392, 83
Coleman, G. D., Wu, C.-C., Weedman, D. W. 1980, ApJS, 43, 393
Conselice, C. J., Bershady, M. A., & Jangren, A. 2000, ApJ, 529, 886
Elmegreen, B. G., et al. 2004, ApJ, accepted (E04)
Eskridge, P. B., et al. 2002, ApJS, 143, 73 (ES02)
El-Zant, A. & Shlosman, I. 2002, ApJ, 577, 626
Friedli, D. & Benz, W. 1993, A&A, 268, 65
Friedli, D. & Martinet, L. 1993, A&A, 277, 27
Hunt, L. K. & Malkan, M. A. 1999, ApJ, 516, 660
Jogee, S., Kenney, J. D. P., & Smith, B. J. 1999, ApJ, 526, 665
Jogee, S., Knapen, J. H., Laine, S., et al. 2002, ApJL, 570, L55
Jogee, S., Scoville, N. Z., & Kenney, J. 2004a, ApJ, submitted (astro-ph/0402341)
Jogee, S., Barazza, F., Rix, H.-W., et al. 2004b, in Penetrating Bars through Masks of Cosmic Dust, eds. D. Block, K. Freeman, R. Groess, I. Puerari, & E.K. Block (Dordrecht: Kluwer), in press (astro-ph/0408267)
Knapen, J. H., Shlosman, I., & Peletier, R. F. 2000, ApJ, 529, 93
Kormendy, J. & Kennicutt, R. C. 2004, ARAA, submitted.
Laurikainen, E., Salo, H., & Rautiainen, P. 2002, MNRAS, 331, 880
Martinez-Valpuesta, I., Shlosman, I. & Heller, C.H. 2004, ApJ, submitted
Martinez-Valpuesta, I. & Shlosman, I. 2004, ApJ Letters, 613, in press (astro-ph/0408241)
Peng, C. Y., Ho, L. C., Impey, C. D., & Rix, H. 2002, AJ, 124, 266
Pfenniger, D. & Norman, C. 1990, ApJ, 363, 391
Regan, M. W., Vogel, S. N., & Teuben, P. J. 1997, ApJL, 482, L143
Rix, H., et al. 2004, ApJS, 152, 163
Sakamoto, K., Okumura, S. K., Ishizuki, S., & Scoville, N. Z. 1999, ApJ, 525, 691
Shen, J. & Sellwood, J. A. 2004, ApJ, 604, 614
Sheth, K., Regan, M. W., Scoville, N. Z., & Strubbe, L. E. 2003, ApJL, 592, L13 (S03)
Shlosman, I., Frank, J., & Begelman, M. C. 1989, Nature, 338, 45
Shlosman, I. & Noguchi, M. 1993, ApJ, 414, 474
Wolf, C., et al. 2004, A&A, 421, 913
Wozniak, H., et al. 1995, A&A Suppl., 111, 115

TABLE 1
OPTICAL FRACTION $f_{\rm opt}$ OF STRONG ($e \geq 0.4$) BARS

Redshift range (1)	$N_{\rm gal}$ (2)	Technique to identify disks/spirals (3)	$N_{\rm sp-disk}$ (4)	Filter to trace bars (5)	Rest-frame band (6)	Optical bar fraction $f_{\rm opt}$ (7)
Method I: Using the reddest ACS filter (F850LP) to identify bars						
0.25–0.70	384 (146)	Sersic n	148 (39)	F850LP	I to V	36% (33%)
0.70–1.0	243 (135)	Sersic n	110 (49)	F850LP	V to B	24% (27%)
0.25–0.70	384 (146)	CAS C	170 (51)	F850LP	I to V	27% (27%)
0.70–1.0	243 (135)	CAS C	147 (73)	F850LP	V to B	23% (23%)
0.25–0.70	384 (146)	$U-V$	175 (51)	F850LP	I to V	29%(28%)
0.70–1.0	243 (135)	$U-V$	139 (69)	F850LP	V to B	29% (26%)
Method II: Using F606W and F85OLP to identify bars at a ~ fixed rest-frame B/V band						
0.25–0.70	384 (146)	Sersic n	148 (39)	F606W	V to B	26% (30%)
0.70–1.0	243 (135)	Sersic n	110 (49)	F850LP	V to B	24% (27%)
0.25–0.70	384 (146)	CAS C	170 (51)	F606W	V to B	24% (28%)
0.70–1.0	243 (135)	CAS C	147 (73)	F850LP	V to B	23% (23%)
0.25–0.70	384 (146)	$U-V$	175 (51)	F606W	V to B	29% (23%)
0.70–1.0	243 (135)	$U-V$	139 (69)	F850LP	V to B	29% (26%)

Note. — Col. (1): The redshift range. Col. (2): The no of galaxies in this range with $M_{\rm V} - 5 \log h \leq -18.5$ and -19.9 (shown in brackets). Ellipses were fitted to these galaxies in order to characterize galactic features such as bars, bulges, and disks. Col. (3): The technique used to identify disk/spiral galaxies from the sample in (2). We use cuts of Sersic index $n < 2.5$, CAS concentration index $C < 3.4$, and rest-frame $U-V < 0.8$–1.2. Col. (4): $N_{\rm sp-disk}$, the no of moderately inclined ($i < 60°$) spiral/disk galaxies for the two magnitude cuts in (2). Col. (5),(6): The filter and rest-frame band in which bars are traced; Col. (7): $f_{\rm opt}$, the optical fraction of strong bars, is the fraction ($N_{\rm bar}/N_{\rm sp-disk}$) of moderately inclined spirals hosting bars with $e \geq 0.4$. Values for the two magnitude cuts of -18.5 and -19.9 are shown.

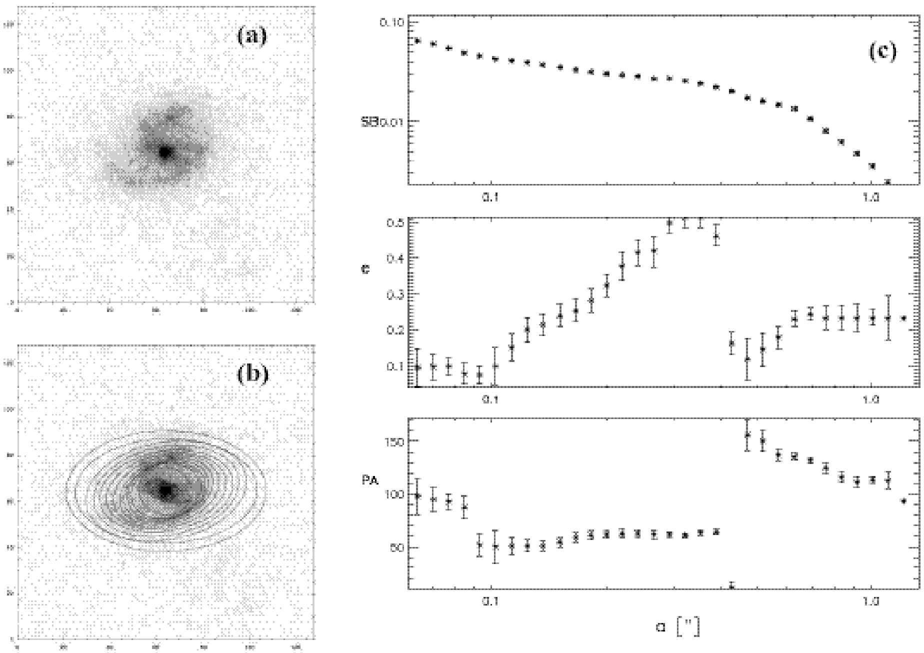

Fig. 1 — Identification and characterization of bars out to $z \sim 1.0$: The GEMS image of a $z \sim 0.5$ galaxy with a bar, prominent spiral arms, and a disk is shown without *(a)* and with *(b)* an overlay of the fitted ellipses. *(c)* In the resulting radial plots of the surface brightness, ellipticity e, and PA, the bar causes e to rise smoothly to a global maximum, while the PA has a plateau over the region dominated by x_1 orbits. Beyond the bar semi-major axis a of $\sim 0.36''$, the spiral arms lead to a twist in PA and varying e. Once the disk dominates, e drops sharply.

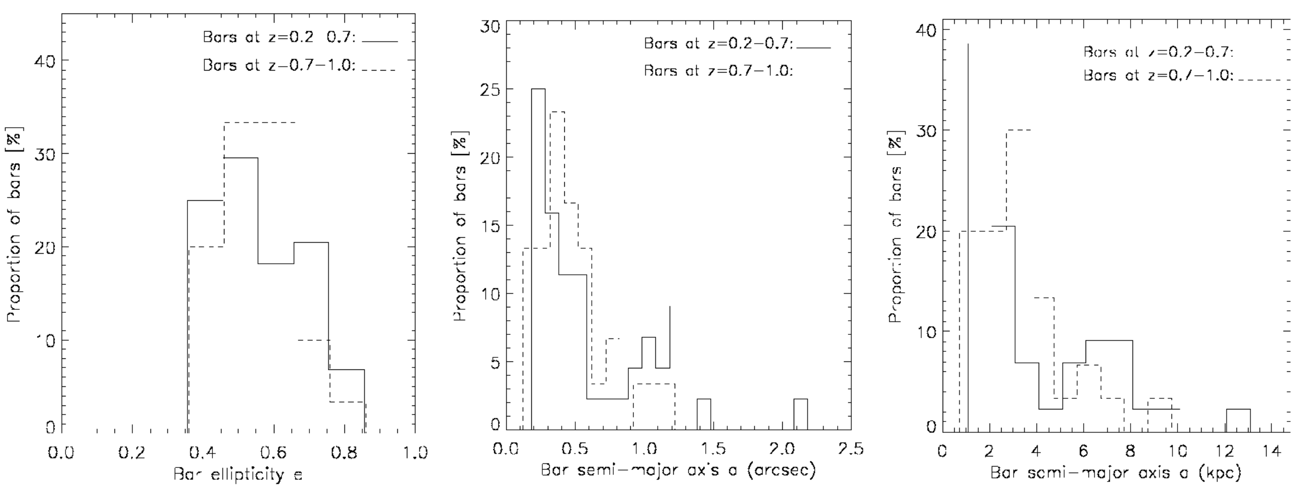

Fig. 2 — Comparison of bars out to lookback times of 8 Gyr: *(a)* The bar ellipticities e, and *(b)*, *(c)* the bar semi-major axes a are shown for bright (M_V - 5 log $h \leq -18.5$), moderately inclined ($i < 60°$) galaxies at $z \sim 0.2$–0.7 ($T_{\rm back} \sim$ 2–6 Gyr) and $z \sim 0.7$–1.0 ($T_{\rm back} \sim$ 6–8 Gyr). The bars identified are primarily strong, with ellipticities $e \geq 0.4$. A large fraction have $a < 0.5''$ and their detection is aided by the narrow ACS PSF.